A Dissertation on

PRE-EQUILIBRIUM STUDIES: A CASE OF $^{12}C+^{175}Lu$ SYSTEM

Submitted in the partial fulfillment of the requirements of the degree of

MASTER OF TECHNOLOGY

In

NUCLEAR SCIENCE & ENGINEERING

By

HIMANSHU PALIWAL

2K14/NSE/11

Under the Guidance of

Dr. Nitin K Puri
Assistant Professor
DTU, New Delhi

Dr. Rakesh Kumar
Scientist 'F'
IUAC, New Delhi

Department of Applied Physics,
Delhi Technological University
(Formerly Delhi college of Engineering)
Govt. of NCT of Delhi
Main Bawana Road, Delhi-110042

YEAR: 2016

Department of Applied Physics

Delhi Technological University (DTU)

(Formerly Delhi College of Engineering, DCE)

Govt. of NCT of Delhi

Bawana Road, Delhi-110042

CERTIFICATE

*This is to certify that the Major project (AP-811) report entitled "***PRE-EQUILIBRIUM STUDIES: A CASE OF $^{12}C+^{175}Lu$ SYSTEM***" is a bonafide work carried out by* **Mr. Himanshu Paliwal** *bearing Roll No.* **2K14/NSE/11**, *a student of Delhi Technological University, in partial fulfilment of the requirements for the award of Degree in* **Master of Technology** *in* "**Nuclear Science & Engineering**". *As per declaration of the student this work has not been submitted to any university/institute for the award of any degree/diploma.*

(**Dr. Nitin K Puri**)

Course Coordinator

Department of Applied Physics,

Delhi Technological University,

Delhi-110042

(**Professor S C Sharma**)

Head of Department

Department of Applied Physics,

Delhi Technological University

New Delhi 110042

INTER-UNIVERSITY ACCELERATOR CENTRE (IUAC)

Aruna Asaf Ali Marg, Near Vasant Kunj

New Delhi, 110067 INDIA

CERTIFICATE

This is to certify that the project entitled "**PRE-EQUILIBRIUM STUDIES: A CASE OF $^{12}C+^{175}Lu$ SYSTEM**", completed by Mr. Himanshu Paliwal, a student of M.Tech., Nuclear Science and Engineering of Applied Physics Department at Delhi Technological University, New Delhi, embodies the original work carried out by him under my supervision and guidance. His work has been found very well for the partial fulfillment of the requirement of the degree of M.Tech. It is further certified that, the student has developed the project during the period of 19th January, 2016 to 9th June, 2016. This report has not been submitted in part or full in any other University for award of any other degree.

Mr. Himanshu Paliwal is a student of good moral character. I wish him success in future.

(**Dr. Rakesh Kumar)**
Scientist 'F'
IUAC, New Delhi
110067

Candidate Declaration

I, hereby declare that the work which is being presented in this thesis entitled "**PRE-EQUILIBRIUM STUDIES: A CASE OF $^{12}C+^{175}Lu$ SYSTEM**" is my own work carried out under the guidance of Dr. N. K. Puri, Assistant Professor, Department of Applied Physics, Delhi Technological University and Dr. Rakesh Kumar, Scientist 'F' Inter University Accelerator Centre, New Delhi. I further declare that the matter embodied in this thesis has not been submitted for the award of any other degree or diploma.

Date: Himanshu Paliwal

Place: New Delhi 2K14/NSE/11

Acknowledgement

First and foremost I would like to thank my parents for their blessings, support and guidance throughout my academic career.

I sincerely thank **Professor S. C. Sharma,** Head of Department, Delhi Technological University for all his support and guidance. His calm attitude and simple nature has always motivated me to how to do any work.

I sincerely convey my thanks to my course co-coordinator and supervisor, **Dr. Nitin K Puri,** for all the support and guidance. Inspiration from him made my work enjoyable and I learned a lot during my master's degree. He has given me valuable insight in many aspects of research. Dr. Nitin K Puri wide knowledge and his logical way of thinking have been of great value in shaping up my dissertation.

I would like to thanks **Dr. Rakesh Kumar** my supervisor at IUAC who has worked day and night with me to complete my dissertation. His great knowledge and experience in the field of Physics help me a lot in doing dissertation. I thank him a lot as under him I had learned many things.

I would also like to thanks **Dr. Vijay R Sharma** (Post Doc.) at IUAC who was with me the entire time ready to help me to complete my dissertation. His support sometimes as a guide and sometimes as an elder brother was wonderful and much required to complete my project in time.

I express my sincere gratitude to all the faculty of Department of Applied Physics. Their moral support and encouragement has played an important part in completion of my master's degree.

I thank all my friends to keep me cheerful and make me smile whenever I feel low.

Himanshu Paliwal

2K14/NSE/11

Dedicated to my parents…

Dedicated to my parents…..

Table of Contents

List of tables

List of figures

Figure 4.4: Experimental xn (x=4) channels populated in $^{12}C+^{175}Lu$ compared with PACE4 code at different k values.

Figure 4.5: Experimental xn (x=5) channels populated in $^{12}C+^{175}Lu$ compared with PACE4 code at different k values.

Figure 4.6: Experimental xn channel (i.e. 3n) populated in $^{12}C+^{175}Lu$ system compared with ALICE91 at different values of COST and K. The rotational energy is not included in the projectile energy.

Figure 4.7: Experimental xn channel (i.e. 3n) populated in $^{12}C+^{175}Lu$ system compared with ALICE91 at different values of COST and K. The rotational energy is included in the projectile energy.

ABSTRACT

The role of pre-equilibrium (PE) emission within the heavy-ion fusion process has not been fully characterized. When two heavy nuclei fuse together, they form a composite nucleus far from the statistical equilibrium, and a large fraction of its energy is considered to be in the form of an orderly translational motion of the nucleons of the projectile and the target nuclei. This orderly motion transforms slowly into chaotic thermal motion through a series of two-body interactions. The thermalization process completes when the composite nucleus reaches a state of thermal equilibrium, referred to as the compound nucleus. As soon as the state of thermal equilibrium is attained, the accumulation of sufficient energy on a single nucleon or a cluster of nucleons may occur in a random sequence of events and hence may require much longer emission times, favoring the emission of low-energy particles. The time scale at which PE emissions occur is very short, $\approx 10^{-21}$ s, while further evaporations from the equilibrated nucleus take a longer time, $\approx 10^{-16}$ s. The rate of emission of the PE nucleons depends on the sensitivity of the mean-field interaction between the projectile and the target nucleus. This determines the initial energy distribution among the nucleons in the projectile and the target nuclei, which starts a cascade of nucleon-nucleon interactions as soon as the two nuclei touch each other.

With a view to study pre-equilibrium emission process, the excitation functions for the neutron emission channel occurring in the fusion of ^{12}C with ^{175}Lu, has been measured at incident energies from near the Coulomb barrier to ≈ 7 MeV/nucleon. The off-line γ -ray spectrometry–based activation technique has been used for the measurements of excitation functions. Further, the measured excitation functions are compared with theoretical predictions based on pure statistical model code PACE4 and Geometry Dependent Hybrid (GDH)-based code ALICE 91. The strength of pre-equilibrium emission is also determined from comparison of the experimental excitation functions and the PACE 4 calculations.

Chapter 1

Introduction

Chapter 1

Introduction

Understanding the fundamental nature of matter has been an exclusive pursuit of scientists since long. The studies in this regard got a great boost, with the discoveries of electron and radioactivity during the last decade of 19^{th} century. Since then, the microscopic world of atomic nucleus has been explored intensively. In an atom, nucleus is a very small entity at the centre and consists of nucleons. The atomic nucleus was discovered, by Rutherford in 1911. The Rutherford-Bohr model of the atom was followed by the advent of quantum mechanics developed by physicists like de-Broglie, Schrödinger, Heisenberg, Pauli, Dirac and others. The consistent efforts on the experimental and theoretical fronts finally led to the present understanding of the nucleus and the atom. In an atomic nucleus, neutrons and protons are held together by strong attractive nuclear forces. Though, information on exact nature of nuclear forces is still limited and not established analytically, however, much progress has been made towards its phenomenological understanding. One way of getting this information is through the study of nuclear reactions. The nuclear reactions may be broadly categorized as elastic and inelastic reactions. In the former, interacting partners only change their direction of motion while in the latter, one or both of the interacting partners may change their internal states along with their nuclear properties. Since, the time scale involved in nuclear reactions is very short ($\approx 10^{-22}$ - 10^{-16} sec), therefore, it is not possible to visualize the process directly. In 1936, Danish physicist, Niels Bohr proposed the description of nuclear reaction on the basis of compound nucleus (CN) theory. According to this theory, nuclear reaction is a two-stage process, (i) the formation of a relatively long-lived intermediate nucleus and its subsequent decay. Here, the incident nucleus loses all its energy to the target nucleus and becomes an integral part of an excited compound nucleus (CN), (ii) After a relatively long period of time ($\approx 10^{-16}$ sec) and independent of the properties of the reactants, the compound nucleus disintegrates, usually into an ejected small particle leaving behind a relatively heavier product nucleus. The CN theory is based on the above description referred to as the 'Bohr's independent hypothesis'. As a

matter of fact, the lapse time between the formation of composite system and its decay is too large, and hence, no trace is left to decide its mode of formation. The validity of independent hypothesis has been experimentally verified by Ghoshal in 1950, where the reaction cross-sections of almost same orders of magnitude (within the experimental uncertainties) have been observed for particular reaction products formed via different entrance channels.

Now a days with the advancement in the nuclear detectors and pulse processing electronics, attempts were made to study the energy spectra, angular distribution and double differential cross-sections of the particles emitted in the nuclear reactions. A typical energy spectrum of charged particles emitted during nuclear reaction, at a given angle, at moderate excitation energy is shown in fig. 1.1

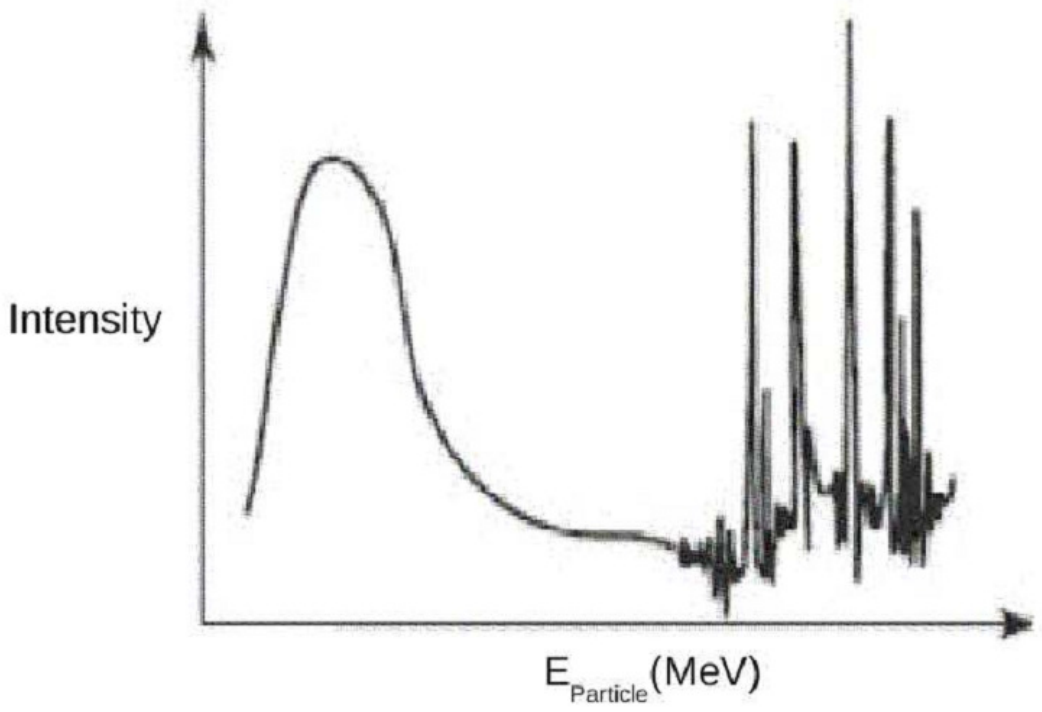

Figure 1.1: Typical spectra of particles emitted in a nuclear reaction at moderate excitation energies

As can be seen from this figure, there lies a broad peak at lower energies followed by the continuum and at relatively higher energies there are several discrete sharp peaks. These isolated peaks at higher energies may be ascribed to the direct reactions, where only few degrees of freedom are involved, while the broad peak at low energies may be energy and angular distributions etc. of particles emitted in nuclear reactions at moderate excitation energies. The broad peak towards the lower excitation energy side can be described to the compound nucleus reaction mechanism while the sharp isolated peaks towards the end of the high energy tail represents the particle production in the direct reaction mechanism. The smooth distribution of particles between the two extremes of the spectrum cannot be explained either by the compound nucleus or the direct reaction mechanisms. It is expected that emission of particles may also takes place during the equilibration of compound system. The particles which are emitted during the equilibration of the compound nucleus is called pre - equilibrium particles, or pre – compound particles and the reaction mechanism is termed as pre - equilibrium emission. Recently it is observed that pre - equilibrium emission mechanism may cause emission of nuclear cluster or even fission also at moderate excitation energies. The pre-equilibrium emission mechanism is featured by slowly descending tails of excitation functions, forward peaked angular distribution of emitted particles and relatively large number of higher energy particles than predicted by the compound nucleus mechanism. Hence the knowledge of excitation functions has served as a good tool for the study of reaction mechanism because the feature of the excitation functions at low, medium and high energies can reveal the reaction mechanism involved. The alpha particles because of their large binding energy are unlikely to break up at moderate excitation energies and as such they are good projectile for the study of reaction mechanism. The measured excitation functions have often been used to examine the reaction models.

With the availability of heavy ion (HI) particle accelerators, one at the Inter University Accelerator Centre (IUAC), New Delhi and the other at the Tata Institute of Fundamental Research (TIFR), Mumbai gave a boost to the study of HI induced fusion reactions in our country. It may be pointed out that, a large number of experimental reports indicate that for heavy ions like ^{12}C, ^{16}O projectile when impigned on medium mass target may produce compound nucleus of high spins via nucleons transfer reactions. . A detailed

discussion on heavy ion induced reactions and how they are different from light ion induced reactions is given in next paragraph.

The term heavy ion (HI) is generally used for the nuclei which are heavier than helium. The HI induced reactions are widely different from light ion induced reactions because of the fact that both the projectile and the target nuclei are many nucleon systems, consequently there is large natural electrostatic repulsion between interacting partners. However, the energy and momentum carried by the HI are relatively large. At energies ≈ a few tens of MeV, heavy ions have wavelength much less than nuclear radii so that in some respect their motion may be considered similar to that of a classical particle ($\lambda << R$). That is why in many cases of heavy ion reactions, the collisions are explained on the basis of classical theory. A typical classical picture of heavy ion collisions is given in Fig. 1.1.

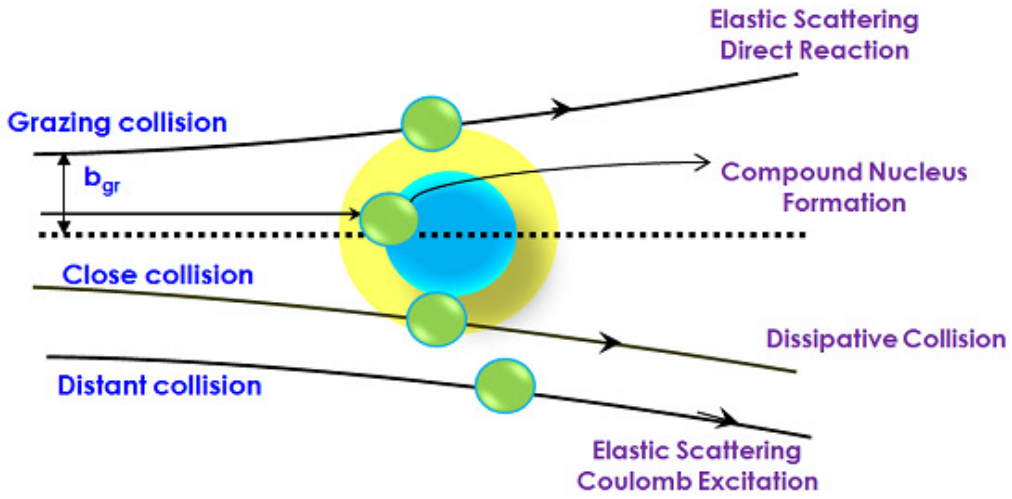

Figure 1.2: Distant, Grazing and close collisions in the classical picture of HI reactions.

According to classical picture, broadly there may be three types of collisions, which may be described on the basis of impact parameter 'b' or the corresponding angular momentum 'ℓ'. As can be seen from fig. 1.2, at projectile energies deep below the fusion barrier (B_{fus}) and at large values of impact parameter 'b', the projectile does not touch the target nucleus and is elastically scattered through the Coulomb field leading to the

'distant collisions'. In such type of reactions, no mass is transferred from the projectile to the target nucleus and/or vice-versa, and the Coulomb forces exclusively determine the process (elastic scattering and/or Coulomb excitation). However, when the projectile and target nuclei come into close contact then the nuclear interactions set in. Meaning thereby, if the impact parameter is comparable to the sum of the radii of the interacting partners, 'grazing collisions' may takes place and the projectile can be elastically or in-elastically scattered. As such, the projectile smoothly grazes along the outer surface of the target nucleus. Moreover, when the projectile interacts with the target nucleus at smaller values of impact parameter with relatively high bombarding energies (just enough to enter in the nuclear field range of target nucleus) then 'deep inelastic collisions' (DIC) dominate. Here, the projectile interacts strongly with the target nucleus. In this region the overlap of the ions is much less than in case of fusion, but it is sufficient to allow a strong interaction between the two ions which transforms a sizeable fraction of kinetic energy into internal excitation energy of two reaction products. In such a case, the nuclear density rises very rapidly in the surface region of target nucleus, and a few nucleons may get transferred from the projectile to the target nucleus, which is also referred to as the 'massive transfer reaction'. Further, if the projectile interacts with the target nucleus very strongly at still smaller values of impact parameters, the projectile completely fuses with the target nucleus resulting into the formation of a composite nucleus which undergoes statistical equilibrium. The typical ranges of impact parameters that may lead to different processes are summarized in Table.1.1. The total cross-section may be related to the values according to the relation;

$$\sigma = \Pi\lambda^2 \ \ell^2 \qquad 1.1$$

where, λ is the reduced wave-length of the incident ions. The fig 1.3, shows the contribution of various l-values towards the total cross-section. In this figure, the values ℓ_{crit} , ℓ_f , ℓ_D and ℓ_{max} represent the limits of the angular momenta for the compound nucleus (CN) formation, fission-like (FL) phenomena, deep inelastic scattering (D) and quasi elastic (QE) reactions respectively. However, the relatively higher ℓ -values contribute towards elastic (EL) scattering and Coulomb excitation (CE). The slanting

long dashed line represents the geometrical partial cross-section and may be given by expression,

$$\frac{d\sigma}{dl}=2\Pi\lambda^2\ \ell \qquad 1.2$$

Vertical dashed lines indicate the extensions of various ℓ -windows in a sharp cutoff model with the characteristics ℓ -values noted at the abscissa. Unshaded areas represent the diffused ℓ -windows assumed in a smooth cutoff model.

Table 1.1 Impact parameter values and angular momentum (ℓ) representing different types of heavy-ion reactions.

Distance of closest approach (r_{min})	**Angular Momentum (ℓ)**	**Type of Nuclear reactions**
b or rmin >RN(=R1+R2)	$\ell > 1\ \ell_N$	Coulomb excitation (Rutherford(elastic) scattering)
$R_F < r_{min} \leq R_{DIC}$	$\ell_{DIC} > \ell > 1\ \ell_N$	Close collision (Deep in-elastic scattering)
$R_{DIC} < r_{min} \leq R_N$	$\ell_N > \ell > \ell_{DIC}$	Transfer reactions (elastic and in-elastic scattering)
$0 \leq r_{min} \leq R_F$	$\ell < \ell_F$	Fusion reaction (Compound nucleus formation)

Here, r_{min} is the distance of closest approach, R_N is the grazing range of nuclear force, R_{DIC} is the minimum distance for the deep inelastic collision, while R_F is the minimum distance for fusion reactions.

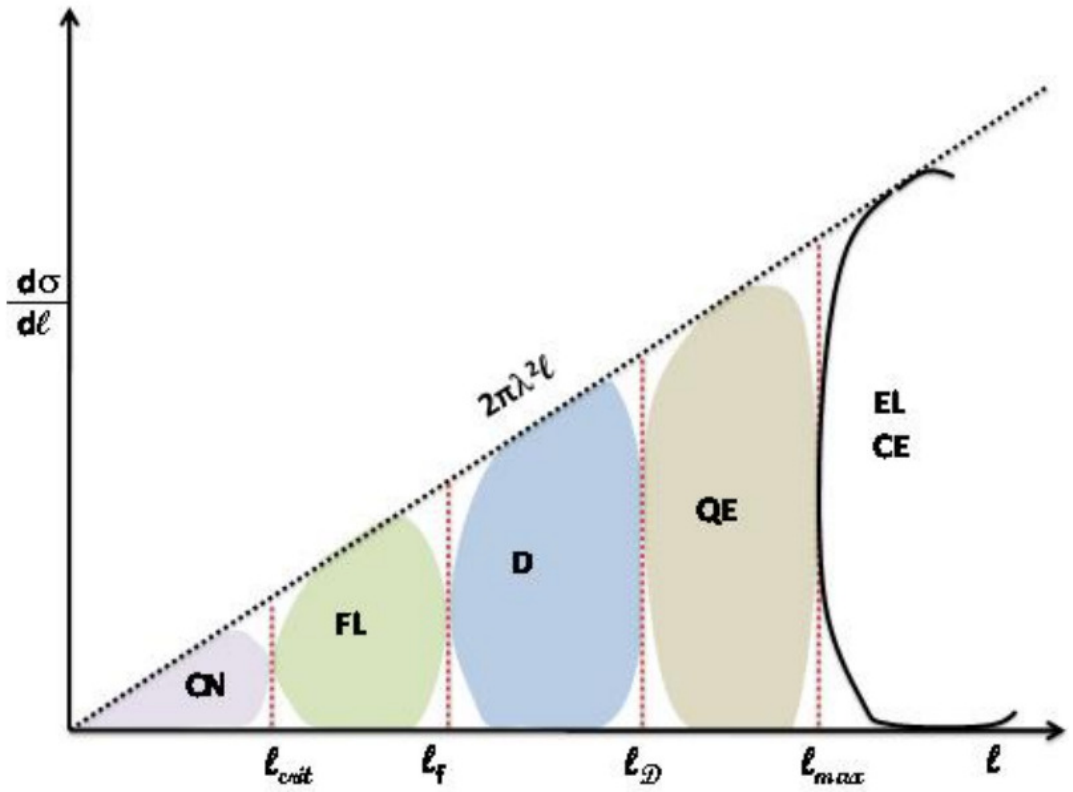

Figure 1.3: Schematic illustration of the reaction probability as a function of entrance channel angular momentum (ℓ).

At present, it is not clear, how large the overlapping regions are for an individual mode of reaction. In the simplest form, one can set an assumption of effective nuclear potential V_{eff} , that depends on the relative separation (r) of two interacting nuclei. The V_{eff} , as a function of 'r' and relative angular momenta 'ℓ' may be written as the sum of Coulomb, nuclear and centrifugal potential terms and may be given as,

$$V_{eff}(r, \ell) = V_{Coul}(r) + V_{nucl}(r) + V_{cent}(r, \ell) \qquad 1.3$$

where, V_{Coul} (r) is the Coulomb potential, V_{nucl} (r) is the nuclear potential and V_{cent} (r, ℓ) is the centrifugal potential. The repulsive Coulomb potential V Coul (r) may be given as,

$$V_{Coul}(r) = \frac{Z1Z2e2}{4\Pi\varepsilon r}; \text{ for } r \geq (R_1 + R_2) \qquad 1.4$$

And

$$V_{Coul}(r) = \frac{Z1Z2e2}{4\Pi\varepsilon r}\left(3 - \frac{r2}{R\,col\,2}\right);\ \text{for } r \leq (R_1 + R_2) \qquad 1.5$$

Here, Z1 and Z2 are the atomic numbers, while, R_1 and R_2 are the radii of the projectile and the target nuclei, respectively. The complex short-range attractive nuclear potential $V_{nucl}(r)$ has been described in different forms. Wood-Saxon form is the simplest form for the nuclear potentials and is given as;

$$V\ nucl(r) = \frac{V0}{1+exp(\frac{r-R}{a})} \qquad 1.6$$

where, $R = r_o\ (A_1^{1/3} + A_2^{1/3})$, V_0 is the depth of the potential and 'a' is the diffuseness parameter. The repulsive centrifugal potential $V_{cent}(r, \ell)$ is given by,

$$V_{cent}(r, l) = \frac{\hbar}{2\mu}\frac{l(l+1)}{r2} \qquad 1.7$$

here, ℓ is the angular momentum and μ the reduced mass of the interacting nuclei. The effective potential V eff (r, ℓ) can be written as;

$$V_{Coul}(r) = \frac{Z1Z2e2}{4\Pi\varepsilon r} + \frac{V0}{1+exp(\frac{r-R}{a})} + \frac{\hbar}{2\mu}\frac{l(l+1)}{r2};\ \text{for } r \geq (R_1 + R_2) \qquad 1.8$$

And

$$V_{Coul}(r) = \frac{Z1Z2e2}{4\Pi\varepsilon r}\left(3 - \frac{r2}{R\,col\,2}\right) + \frac{V0}{1+exp(\frac{r-R}{a})} + \frac{\hbar}{2\mu}\frac{l(l+1)}{r2};\quad \text{for } r \leq (R_1 + R_2) \qquad 1.9$$

where, the terms used have their usual meanings. It may be observed that the magnitude of μr^2 strongly affects the contribution of the centrifugal potential to the effective interaction potential for each partial wave. As a representative case, the effective potential V eff (r, ℓ) for $^{12}C + ^{175}Lu$ system, as a function of relative separation (r) between interacting ions is shown in fig 1.4, for different ℓ - values. In this figure 'r' is the distance of closest approach which is related to the impact parameter 'b' by the relation

$$r = \frac{b}{\sqrt{1-\frac{V(r)}{Ecm}}} \qquad 1.10$$

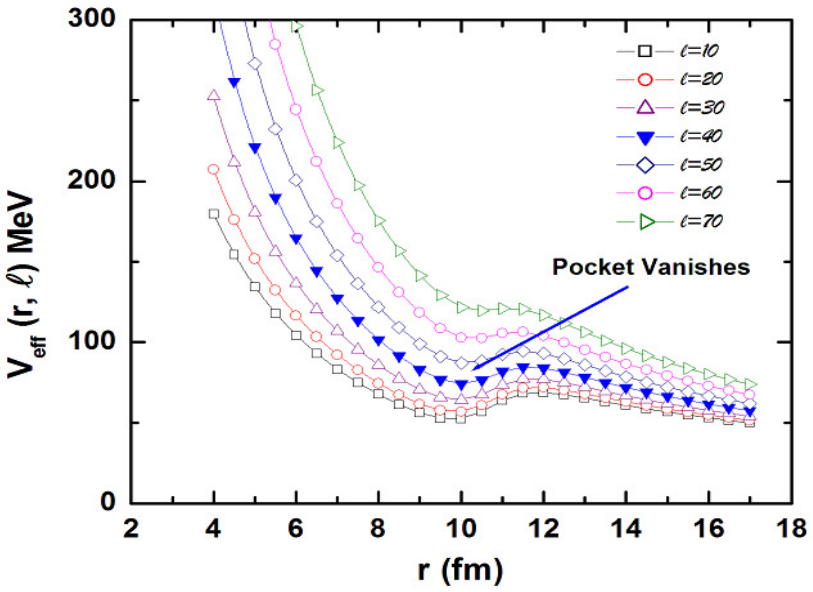

Figure 1.4 Graph of Effective potential $V_{eff}(r, \ell)$ as a function of relative separation "r" between the interacting ions for the system $^{12}C + ^{175}Lu$.

As has already been discussed that no systematic study of pre-equilibrium emission from the excitation functions has been done so far. Also there are large discrepancies in the cross section values reported by different workers for the same reaction. With the aim of studying pre-equilibrium emission in a consistent and systematic way an attempt is made to reinvestigate the neutron channels of the $^{12}C + ^{175}Lu$ system. Measurement of excitation functions for the neutron exit channels has been done using stacked foil activation technique. Experiments was performed at the Inter University Accelerator Centre (IUAC) New Delhi. The post irradiation analysis has been carried out using a high resolution HPGe detector coupled to the multichannel analyzer. The measured excitation

functions have been theoretically calculated and analyzed to study the relative contribution of the equilibrium and pre equilibrium parts of the reactions. The theoretical calculations have been done using computer codes ALICE-91 and PACE4. It may be pointed out that PACE4 do not predict pre-equilibrium cross-section. The equilibrium part of the analysis has been done using Hauser-Feshbach/Weisskopf-Ewing model while, the pre-compound contributions are stimulated employing excitation model/hybrid model respectively. A significant amount of pre-compound contribution to the reaction process for the 3n channel has been observed. ^{175}Lu(^{12}C,3n)^{184}Ir, ^{175}Lu(^{12}C, 4n)^{183}Ir and ^{175}Lu(^{12}C, 5n)^{182}Ir.

The details of the experimental measurements are described in chapter 2 and the theoretical models are briefly summarized in chapter 3 of the thesis. The 4th chapter deals with the measurement of cross-sections, the results and conclusions of the present measurements. References are presented in the end of thesis.

CHAPTER 2

EXPERIMENTAL DETAILS

CHAPTER 2

EXPERIMENTAL DETAILS

The experiments reported in this dissertation have been carried out, using the 15UD Pelletron accelerator, at the Inter University Accelerator Centre (IUAC), New Delhi, India. Brief details of this accelerator are described in section 2.1. Details of the activation technique used for measuring the cross-sections of the reaction products are given in section 2.2. The method of the sample preparation, for the measurement of cross-sections used to obtain the fission fragment mass distribution and isotopic yield of residues populated via complete fusion (CF) and/or incomplete fusion (ICF), are presented in section 2.3. The method of irradiation of the samples is presented in section 2.4, while the post irradiation analysis including the calibration and efficiency determination of High Purity Germanium (HPGe) spectrometer are described in section 2.5.

2.1 15UD PELLETRON ACCELERATOR

A particle accelerator is one of the most versatile instruments, used to study the nature of the matter and energy. The IUAC, New Delhi, Pelletron is a 15UD, tandem electrostatic accelerator and is capable to accelerate any ion (independent of its mass and charge state) from proton to Uranium in the energy region from a few tens of MeV to a few hundred MeV, depending on the ion species. The accelerator is installed in a vertical configuration in a huge stainless steel tank of 26.5 meter in height and 5.5 meter in diameter. The tank is filled with a high di-electric constant gas SF 6 at ≈ 7-8 atmospheric pressure to insulate the high voltage terminal from the tank wall to prevent the breakdown of high voltage. In the middle of the tank there is a high voltage terminal, which can hold potential upto 16 million volts (MV). Since, 16MV is quite high a potential, special technique of charging the terminal is adopted using the pelletron charging chain. The basic principle of acceleration of charged particles with this accelerator is similar to that of Van de Graff generator, except a novel feature that it uses the accelerating voltage twice and hence the name tandem accelerator. Once the terminal is charged to a high voltage, it may be used

for accelerating any ion beam. A typical layout of Pelletron setup is shown in Fig. 2.1. By attaching an extra electron to the neutral atoms, negative ions are produced in the ion source. The negative ions are injected at the ground potential to the accelerator with the help of an injector magnet and the beam is accelerated towards the terminal at high positive potential, increasing its energy to eV_t (where, V_t is the terminal potential in million volts). At the terminal, these ions pass, either through a thin carbon foil or some gas used as stripper, which strips-off at least few electrons from each negative ion, thereby, converting them to positive ions. Since, the terminal is at high positive potential, the positive ions formed after stripping are now repelled and accelerated below the terminal to ground potential. If the charge state of positive ion after passing through the stripper at the terminal is q, then the energy gained in the acceleration below the terminal to the ground potential is qV_t . Therefore, after passing through the two stages of acceleration the final energy of the ion beam is given by,

$$E_{final} = E_0 + (q + 1)V_t \text{ MeV}$$

where, E_0 is the energy of the ion before acceleration by terminal voltage V_t and q is the charge state of ion after stripping. Since, $E_0 << E_{final}$, it may be neglected. As such, the above equation may be written as;

$$E_{final} = (q + 1)V_t \text{ MeV}$$

These high-energy ions are then passed through the analyzing magnet and energy slits which selects the particular ions of the desired energy. With the help of switching magnets the beam of ions is then directed towards the desired experimental area. A schematic diagram of different beam lines at the IUAC, New Delhi Pelletron facility is shown in Fig. 2.2.

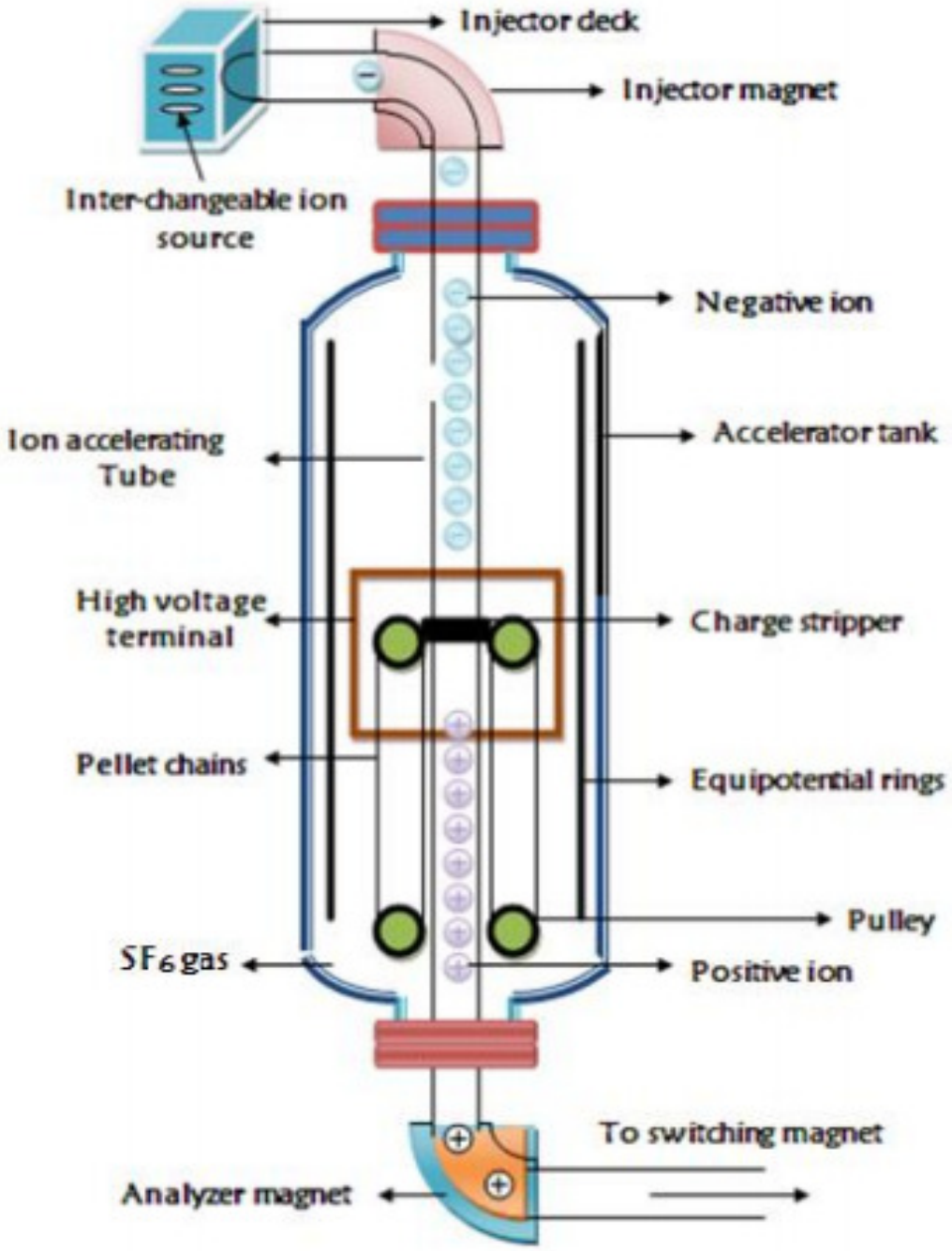

Figure 2.1: A schematic diagram of the IUAC Pelletron.

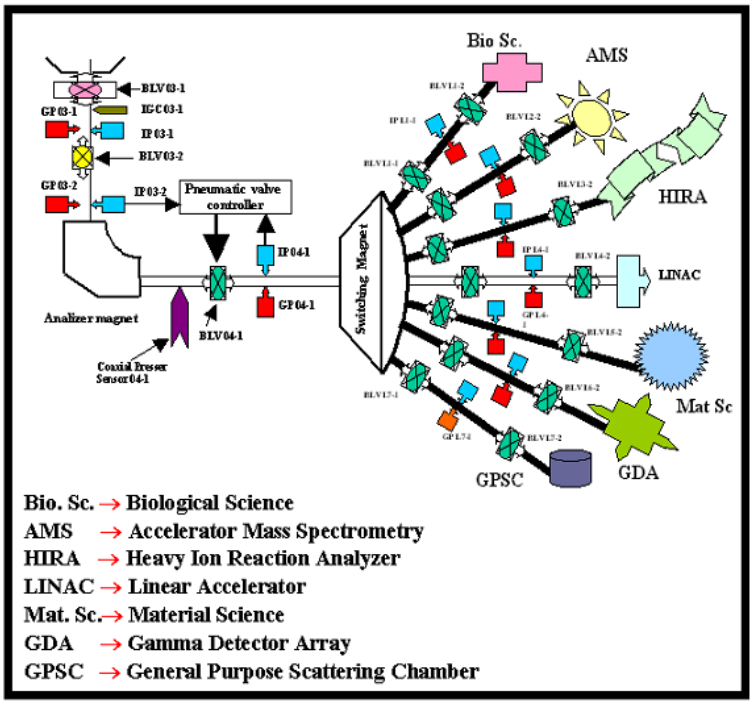

Figure 2.2: A schematic diagram of different beam lines at IUAC pelletron facility.

2.2 STACKED FOIL ACTIVATION TECHNIQUE

In the present work, stacked foil activation technique has been used for the measurement of cross-section of the residues populated in various processes. It may be emphasized that activation technique is a non destructive method of measuring concentration of constituents in a given sample by measuring the characteristic radiations emitted by the radioactive nuclides resulting from selected nuclear transformations. Activation technique is one of the simplest and powerful methods for measuring the cross-section of the nuclear reactions and to deduce important information about the reaction dynamics. In this technique, a stack of targets backed by suitable catcher/degrader foils is irradiated by an energetic beam. After the irradiation, the activities induced in the target-catcher foil assembly are recorded off- line for a considerably long time depending on the half-lives of reaction products of interest. Some of the important advantages of the activation technique are given below;

• When a sample is irradiated, several nuclear reactions may take place simultaneously. Many of these reactions produce radioactive nuclides. Each radioactive nuclide has its characteristic half-life and decay mode. The technique provides the possibility of measuring cross-sections for several reactions at different projectile energies in a single irradiation, hence the beam-time requirements may be minimized.

• Measurement of induced activity may be done after the irradiation. Therefore, there is no possibility of contamination from the beam background, and the spectrum becomes quite clear.

• With the availability of high resolution semi-conductor detectors, it is now possible to separate out the activities of different reaction products emitting γ-rays of nearly same energies quite accurately. As a result, errors in the measurements are expected to be quite low. Further, often a given radio-active residue emits gamma rays of more than one energy. By measuring the intensities of these radiations, cross-section for the production of the residue can be determined in a self consistent way. Though, activation technique is quite simple and accurate but sometimes it becomes complicated due to the presence of radiations (γ-rays) of almost similar energies for more than one reaction products. In case of mixing of nearby γ-rays due to different isotopes, the contribution of each isotope can be separated out by decay curve analysis. The unique half-life of each radioactive isotope provides a specific way for its identification and measurement. It may, however, be pointed out that this technique is limited only for the reaction products having measureable half-lives.

2.3 SAMPLE PREPARATION

In the present work, self supporting samples of isotropically pure ^{175}Lu (99.99%) of thickness ≈ 1.5 mg/cm2 have been prepared by rolling method and were pasted on Al-catcher foils (also prepared by rolling method) of thickness ≈ 2.0 mg/cm2. A typical photograph of the machine at IUAC, New Delhi used for rolling the samples is shown in Fig. 2.3. The thickness of the Al-catcher was chosen keeping in view of the fact that even the most energetic residues produced due to complete momentum transfer may be trapped in the catcher thickness. Further, the thicknesses of each sample and the catchers were

measured by α-transmission method in which 5.485 MeV α-particles obtained from ^{241}Am source were allowed to pass through the sample foil to estimate the energy loss in the sample while traversing the sample materials.

Figure 2.3: The rolling machine used for the preparation of thin samples and catcher foils at the target laboratory of IUAC.

A block diagram of experimental setup used for the thickness measurements of samples and catcher foils is shown in Fig. 2.4.

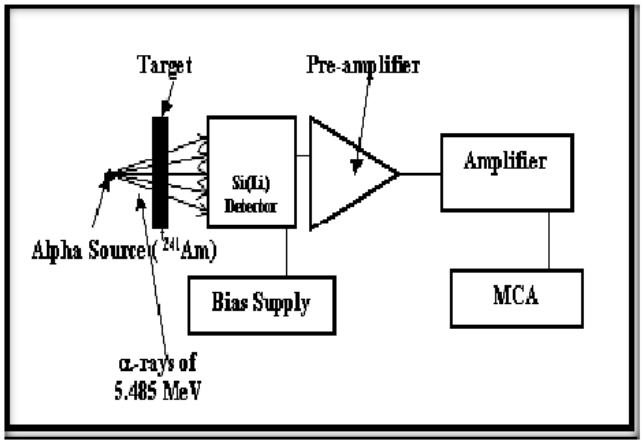

Figure 2.4: A typical block diagram of the setup used for the thickness measurements.

It may however, be pointed out that the source, the sample whose thickness is to be determined and the Si(Li) detector are kept in a vacuum chamber. During the irradiation, the Al-backing of targets served both as energy degrader as well as catchers for the residues recoiling out of the target foil during the irradiations. The samples were cut into the size of 1.2 × 1.2 cm2 and were pasted on Al-holders having concentric hole of 1.0 cm. The Al-holders have been used for rapid dissipation of heat produced during the irradiation.

2.4 IRRADIATION

Irradiations were performed in the General Purpose Scattering Chamber (GPSC) of 1.5 m diameter having an in-vacuum transfer facility (ITF) using conventional recoil catcher technique. Using this ITF facility the samples after irradiation may be changed in the GPSC without disturbing the vacuum inside the chamber. Thus, the time lapse between the stop of the irradiation and the counting of the samples may be considerably reduced and thus induced activities of short half-lives may be recorded. Typical photographs of GPSC and ITF are given in Figs. 2.5 (a) and (b), respectively.

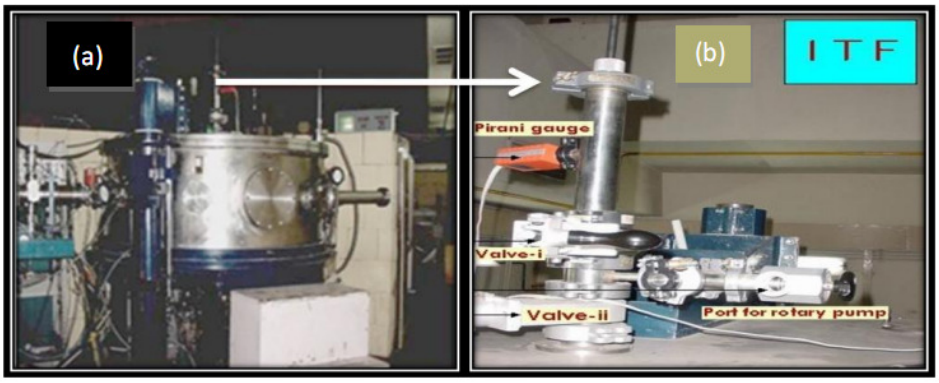

Figure 2.5: (a) The general purpose scattering chamber (GPSC), (b) typical arrangement of an in-vacuum transfer facility (ITF), used for in-vacuum transfer of irradiated samples.

The flux of the incident ^{12}C-ions was monitored using an ORTEC current integrator, by taking into account the total charge collected in the Faraday cup, placed behind the target-catcher foil assembly. In an auxiliary experiment the two silicon surface barrier

detectors D_1 and D_2 (Rutherford monitors) were kept at 300 with respect to the direction of the beam at the forward angles, to record the scattered incident ions for flux determination. Flux of incident ion beam determined from the counts of Rutherford monitors and from the integrated counts of Faraday cup were found to agree with each other within 5%.The samples of ^{175}Lu along with appropriate catcher foil were irradiated at ≈ 97 and 100 MeV beam energies. As the incident beam passes through the stack, it loses its energy both in the target material and in the Al-catcher. As such, successive targets of the stack get irradiated at five different beam energies viz 67MeV, 70MeV, 77MeV, 82MeV and 84MeV. The energies of the incident ion on successive targets have been calculated using stopping power values obtained from code SRIM based on the range-energy formulations. During the irradiation, the samples along with Al-catchers were placed normal to the beam direction, so that the recoiling products could be trapped in the catcher foil placed just behind the target and there would be no loss of activity. Keeping in view the half-lives of interest, irradiations were carried out for ≈ 8–10 hrs duration. The Pelletron crew provided a constant beam current ≈ 3-4 nA throughout the irradiations.

2.5 POST IRRADIATION ANALYSIS

After the irradiation, target-catcher assembly was taken out from the GPSC employing ITF assembly. In order to identify the characteristic γ-rays of residues in the complex γ-ray spectrum, a detector of good resolution with proper calibration is required. The post irradiation analysis has been carried out using a γ-ray spectrometer with a pre-calibrated HPGe detector of 100 c.c. active volume coupled to a PC through CAMAC based CANDLE software. The HPGe detector was pre-calibrated both for energy as well as efficiency by using various standard γ-sources i.e., ^{22}Na, ^{60}Co, ^{133}Ba, ^{137}Cs and ^{152}Eu of known strengths. A list of prominent γ-rays of the standard ^{152}Eu source used in the present measurements are given in Table 2.1. The geometry dependent efficiency (Gε) of the HPGe detector at a given energy has been determined using the following expression;

$$G\epsilon = \frac{N0}{Nm \exp(-\lambda t) Iy} \tag{2.3}$$

where, N_o is the disintegration rate of the standard γ-source at the time of measurement, N_m is the disintegration rate at the time of manufacture of the source, λ is the decay constant, t is the time elapsed between the manufacture of the source and the start of the counting, and I_y is the branching ratio of the characteristic γ-ray. Further, the spectrometer resolution was ≈ 2 keV for 1.33 MeV γ- ray of ^{60}Co source.

Typical geometry dependent efficiency of the spectrometer, as a function of γ-ray energy at 2cm source-detector separation is shown in fig. 2.6. The geometry dependent efficiency curve is found to be best fitted with a 5th order polynomial function of the type;

$$G\epsilon = a_0 + a_1E + a_2E^2 + a_3E^3 + a_4E^4 + a_5E^5 \quad (2.4)$$

where, E is the energy of the γ-ray and a_0, a_1, a_2, a_3, a_4 and a_5 are the coefficients having different values for each source-detector separation. In the present work, the standard γ sources used for efficiency determination and irradiated target-catcher for assemblies were counted in the same geometry in order to avoid the errors due to solid angle effect. Attention was paid to keep the dead time of the detector ≤10% by suitably adjusting the source-detector separation for each irradiated sample.

Table 2.1: A list of γ-ray energies and intensities of the prominent γ-rays from standard ^{152}Eu source.

Eγ ray energy (keV)	**Absolute Intensity (%0**
121.78	28.58
244.69	7.58
344.27	26.54
443.96	2.82
778.90	12.94
867.37	4.24
964.07	14.60
1089.73	1.72

1112.07	13.64
1212.94	1.42
1299.14	1.62
1408.00	21.00

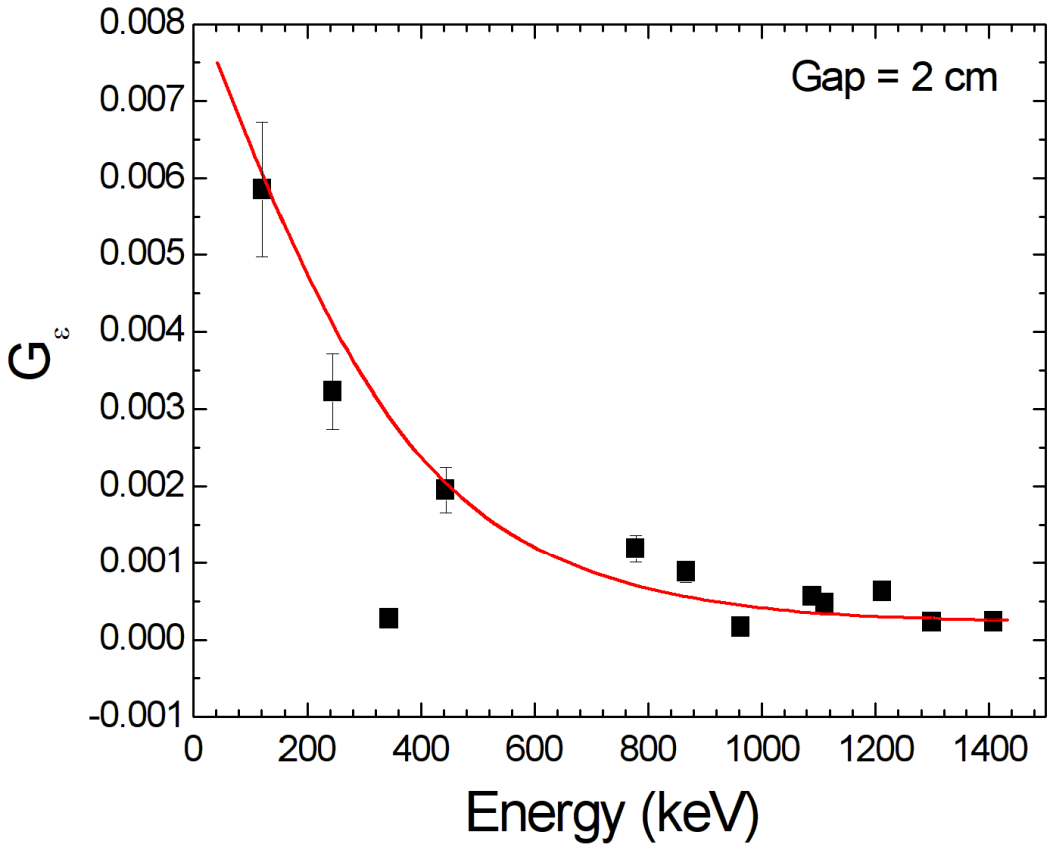

Figure 2.6: The geometry dependent efficiency curve as a function of γ-ray energy at 2cm source-detector separation. Solid lines represent the best polynomial fit.

The measurement of cross-section for the identified neutron channels will be discussed in chapter 4. On the other hand, the therotical model used in the present work are summarized in the next chapter 3.

Chapter 3

Theoretical model description of PACE4 and ALICE91

Chapter 3

Theoretical model description of PACE4 and ALICE91

A compound nuclear reaction is said to be occur only if the projectile bring closer to the target nuclei of laboratory energy greater or equals to Coulomb barrier. The excited nucleus further decays by particle emission followed by γ emission or by process of fission. As a matter of fact, the analysis of a complex interaction such as the compound nucleus formation and its subsequent decay could only be explained through the application of statistical theory. Now-a-days subsequent amount of models/codes are available to understand the dynamics of compound nucleus viz., CASCADE, SUMRULE, PACE4, ALICE91, etc. The following section deals with the brief description of PACE4 and ALICE91 codes.

3.1 PACE4 (Projection of Angular Momentum Coupled to Evaporation Residues)

The statistical model code Projection Angular Momentum Coupled Evaporation (pace4) is derived from the original code JULIAN. It uses a Monte-Carlo procedure to determine the decay sequence of an excited nucleus using the Hauser-Feshbach formalism. Correlations between various quantities such as particles and gamma rays or angular distribution of particles are provided by Monte-Carlo calculations. Sequential decays are considered until any further decay is prohibited due to the energy and angular momentum conservation laws. A random number is selected which determines the actual final state to which the nucleus decays to and the process is, then repeated for other cascades until all the nuclei reach the ground state. The transmission coefficients for light particle emission (n, p, α) are determined using optical model potentials. A fission decay mode is employed using a rotating liquid drop fission barrier routine. The code also provides event by event trace back of the entire decay sequence from the compound nucleus into any one of the exit channels.

The fusion cross-sections are obtained from the Bass model. There are two default level density options that are essentially derived from the Fermi gas formalism and are identical to constant temperature formalism at low energies. These are i) the determination of the parameter 'a' and ii) 'a' is taken to be equal to A/K, where, A is the number of nucleons and K is constant factor. Independent of these options, rotational energy contribution $E_{rot}(J)$ can be selected in two ways viz., the spin cut-off parameter and the ground-state rotational energy of the finite-range rotating-drop model. For values of A, Z or J beyond the range of validity of Sierk's routine, the rotational energies are taken from the work of Cohen, Plasil and Swiatecki. It has been observed that the code PACE4 is more accurate for high spins, close to the yrast line. The fission probability is calculated using the Bohr-Wheeler saddle point formalism. The fission barriers are those of Sierk. The code cannot be used for below barrier calculations. A special feature of the PACE4 code is its ability to provide information on energy and angular distributions of evaporated particles. This is obtained by tracking the distribution of projection through each cascade. The angular distribution of the emitted particles is determined at each stage of de-excitation. The code could be run with a large number of events (50,000) to obtain better statistics for the energy and angular distribution of residual nuclei.

The partial cross-section for CN formation at angular momentum (ℓ) and specific bombarding energy is given by,

$$\sigma_\ell = \frac{\pi\lambda^2}{4\pi^2}(2\ell+1)T_\ell \tag{3.1}$$

where, λ is the reduced wavelength and T_ℓ, the transmission coefficient given by,

$$T_\ell = \left[1+\exp(\ell-\ell_{max})/\delta\right]^{-1} \tag{3.2}$$

where, δ is the diffuseness parameter and ℓ_{max} is determined by the total fusion cross-section σ_F, since,

$$\sigma_F = \sum_{\ell=0}^{\infty} \sigma_\ell \qquad (3.3)$$

It may be pointed out that code PACE4 performs only the statistical equilibrium model calculations and does not take pre-equilibrium (PE) and in-complete fusion processes into consideration.

3.2 ALICE-91

The code ALICE-91 is based on the Weisskopf-Ewing model for compound nucleus reaction. The pre-equilibrium emission is simulated within the framework of Hybrid/Geometry Dependent Hybrid Model. In this code the possibility of only complete fusion is taken into account but it can compute statistical fission cross-sections using Bohr-Wheeler approach. The code considers the emission of neutrons, protons, deuterons and/or α-particles. The code may calculate the reaction cross-sections for the residual nuclei upto 11 mass and 9 atomic number units away from the compound nucleus. Myers-Swiatecki/Lysekil mass formula is used for calculating Q-values and binding energies of all the nuclei in the evaporation chain. The inverse reaction cross-sections used in the code are calculated using the optical model subroutines. The parabolic model of Thomas is used to calculate the transmission coefficients for heavy ions. The pre-equilibrium calculations in this code are done assuming equipartition of energy among the initially excited particles and holes. The important input parameters required in this code are, the level density parameter a, the initial exciton number n_o and the mean free path (MFP) multiplier COST. The MFP for intra-nuclear transitions may be calculated from the optical model of Becchetti and Greenlees or from Pauli corrected nucleon-nucleon cross-sections. The MFP multiplier COST is used to adjust the nuclear mean free path in order to reproduce the experimental data. It accounts for the difference, if any, between the calculated and the actual MFPs for two-body residual interactions. Level densities of the residues may be

calculated either from the Fermi gas model or from the constant temperature form. The Fermi gas model gives,

$$\rho(U) = (U-\delta)^{-5/4}\, e^{2\sqrt{a(U-\delta)}} \tag{3.4}$$

where, δ is the pairing term and U is the excitation energy of the nucleus. The level density parameter a is taken as A/K, where, A is the mass number of the nucleus and K is an adjustable parameter. The level density ρ(U) in constant temperature approach is given as,

$$\rho(U) \propto \frac{1}{T}\varepsilon^{U/T} \tag{3.5}$$

The differential cross-section for emitting a particle of type ν with channel energy ε may be written as;

$$\frac{d\sigma}{d\varepsilon_\upsilon} = \frac{\pi\lambda^2}{4\pi^2}\sum_{I=|0|}^{\infty}(2I+1)T_I\,(2S_\upsilon+1)\sum_{\ell=|0|}^{\infty}T_\upsilon^{\ell}(\varepsilon)\sum_{J=|I-\ell|}^{I+\ell}\rho(\varepsilon,J)/D \tag{3.6}$$

where, λ is the de-Broglie wavelength of the incident ion, T_ℓ the transmission coefficient of the ℓ^{th} partial wave of the incident ion, ρ(ε,J) the spin dependent level density for the residual nucleus, D the integral of numerator over all particles and emission energies, ε the excitation energy of the compound nucleus. S_ν is the intrinsic spin of the particle ν, $T_\upsilon^{\ell}(\varepsilon)$ is the transmission coefficient for the particle ν with kinetic energy ε and orbital angular momentum ℓ.

In the Weisskopf-Ewing calculations, the nuclear moment of inertia is assumed to be infinite and hence there is no energy tied to rotation. As such, there is no level density cut-off at high spin. This code does not take into account the angular momentum involved in heavy ion reactions. However, the heavy ion projectile imparts large angular momentum to the composite system which has a finite moment of inertia.

Hence, the composite nucleus has large rotational energy. Due to nuclear rotation, a nucleus with a given angular momentum J, cannot have energy below a minimum value E_J^{min}, which is given by,

$$E_J^{min} \approx J(J+1)\frac{\hbar^2}{2I} \tag{3.7}$$

here, I being the moment of inertia of the composite nucleus.

If in the last stages of nuclear de-excitation, higher angular momentum of the nucleus inhibits particle emission more than it does γ-emission, then the peak of the excitation functions corresponding to particle emission mode will be shifted to higher energy. A similar shift may also be produced if the mean energy of the evaporated particles increases with increasing nuclear spin. One way of obtaining an estimate of the overall energy shift is from the nuclear rotational energy. Assuming the excited nucleus to be the rigid body, the rotational energy may be given by $E_{rot} \approx (m/M)E_{lab}$, where, m/M is the ratio of the projectile and target masses and E_{lab} is the incident energy. To account for the large angular momentum imparted to the composite system in heavy ion reactions, it is desirable to shift the energy axis of excitation functions calculated with code ALICE-91, by the amount of the rotational energy E_{rot}.

The above discussed models are used to calculate the cross-section of compound nucleus and/or pre-equilibrium cross-sections. In the next chapter identification of reaction residues and measurement of experimental cross-section is discussed where a comparison of theoretical calculation with experimental results is presented.

Chapter 4

Measurement of cross-section

Chapter 4

Measurement of cross-section

4.1 IDENTIFICATION OF NEUTRON CHANNELS

It has already been discussed that the excited composite systems populated may de-excite by emitting the light nuclear particles followed by characteristic γ radiations. A typical γ-ray spectrum produced in 78.36±1.08 MeV ^{12}C induced reactions on ^{175}Lu is shown in Fig. 4.1

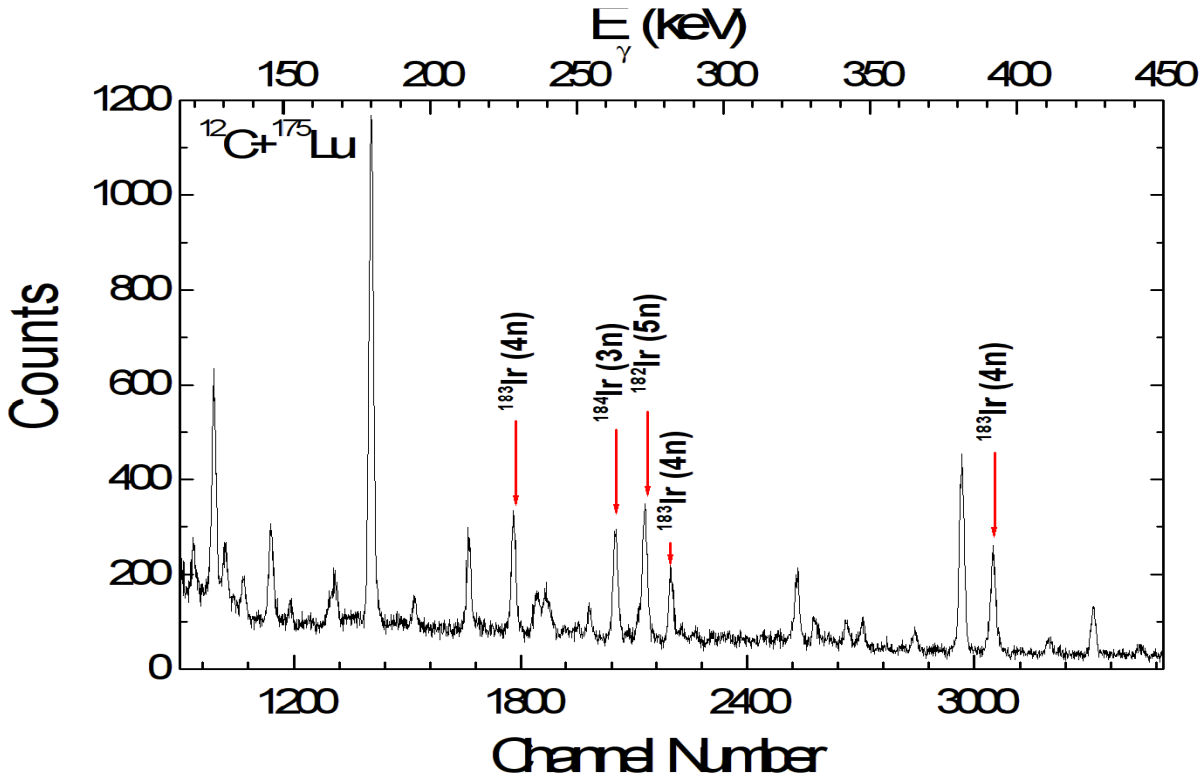

Figure 4.1: A typical γ-ray spectrum produced in $^{12}C+^{175}Lu$ at 78.36±1.08 MeV projectile energy.

The various peaks in observed γ-ray spectra have been assigned to the different radio nuclides (i.e. xn channels) populated via complete fusion (CF) and/or pre-equilibrium

reactions. The preliminary identification of these reaction channels have been done from their observed characteristics γ-rays, which were further confirmed from the decay curve analysis. As such, decay curve analysis is a very specific way for the identification of reaction products, because each radio-active isotope has a unique decay mode. Thus, the observed intensity of the identified γ-ray is a measure of the production cross-section of that particular reaction channel. Since, there were several residues which may emit γ-rays of nearly same energy therefore the simple γ-ray energy identification may not be enough and hence, the intensity of the photo-peaks were plotted as a function of time to get the half-lives of the residues. As a typical example, Figs. 4.2, show the observed decay curve for one of the Iridium isotopes ^{184}Ir(3n) at 80.7±0.91MeV.

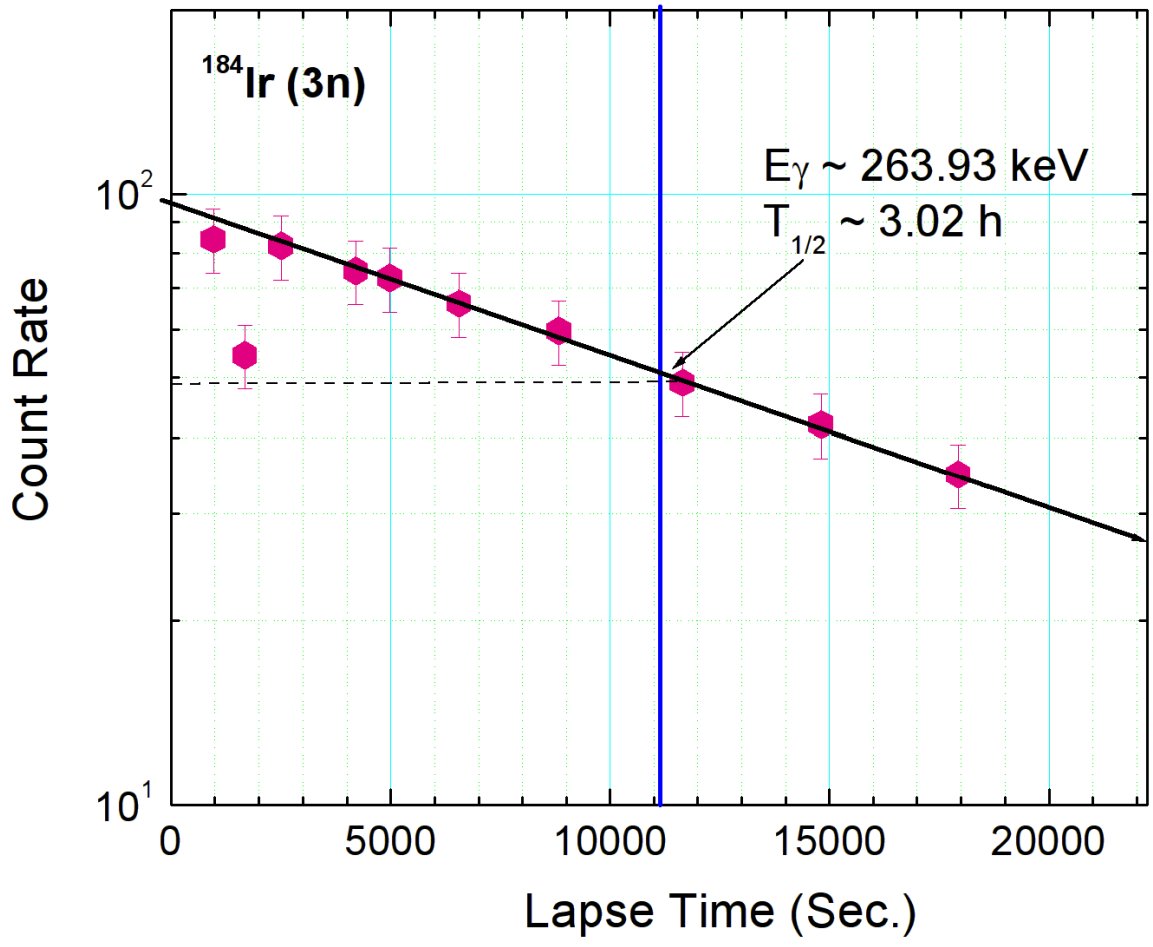

Figure 4.2: Decay curve for one of the Iridium isotopes ^{184}Ir(3n).

Nuclear data like half-lives, γ-ray energies, etc., have been taken from the standard Table of Isotopes and Nuclear Wallet Card. Further the gamma peaks are marked by red downwards arrows are shown in Fig. 4.1, have been assigned to the Iridium isotopes i.e. $^{187-x}$Ir (x=3,4,5). The identified neutron channels in the present work are listed in Table 4.1, along with their spectroscopic properties. It may be mentioned that half-lives of identified residues determined in the present work were found to be in good agreement with the literature values. Data analysis was performed using CANDLE software which is developed at IUAC New Delhi.

Table 4.1: Relevant nuclear data of the reaction residues identified in ^{12}C+^{175}Lu system

Reactions	Residues	Half-life	J^{π}	E_{γ} (keV)	I_{γ} (%)	Mode
^{175}Lu(^{12}C, 3n)	^{184}Ir	3.02 h	$5/2^-$	119.77 263.95 390.37 961.19	30.3 67.5 25.7 12.4	E ε ε ε
^{175}Lu(^{12}C, 4n)	^{183}Ir	57 m	$5/2^-$	228.5 282.4	100[a] 70[a]	- -
^{175}Lu(^{12}C, 5n)	^{182}Ir	15 m	5^+	273.09	43	E2

[a] relative intensities

4.2 MEASURED CROSS-SECTIONS

In the present work, an attempt has been made to measure the cross-sections for the neutron channels produced in the interaction of ^{12}C+^{175}Lu at 4-7 MeV/A beam energies respectively. It may be relevant to mention that the present experiment was performed using offline technique which is also called activation technique because of the fact that this method is used to analyze the activity of the residual nucleus in the nuclear reaction. Further the counting of the irradiated samples done after the stop of the beam. The formulation used for the determination of production cross-section

is discussed below. The irradiation of a sample by the particle beam may initiate various reactions in it, and many isotopes are likely to be formed by the process of transmutation. The rate of formation *N,* of a particular activation product may be given by the expression,

$$N = N_0 \Phi \sigma_{X(a,b)} \tag{4.1}$$

where, Φ is the flux of incident beam, N_0 is the initial number of nuclei in the sample, and $\sigma_{X(a,b)}$ is the reaction cross-section for that particular channel.

$$\sigma_{X(a,b)}(E) = \frac{Number\ of\ events\ X(a.b)Y/area}{N_0 \Phi\ t} \tag{4.2}$$

a is incident particle

X is target nucleus

b is emitted particle

The disintegration rate of the induced activity in a sample after a time '*t*' from the stop of irradiation may be given as;

$$\left[\frac{dN}{dt}\right]_t = N \frac{[1-e^{(-\lambda t_1)}]}{e^{(\lambda t)}} \tag{4.3}$$

where, t_1 is the time of irradiation and λ is the decay constant of the induced activity given as;

$$\lambda = \frac{\ln 2}{t_{1/2}} \tag{4.4}$$

The factor $[1- exp(-\lambda t_1)]$ takes care of the decay of residues during the irradiation and is typically known as the saturation correction. The number of decays of the induced

activity in a very small time '*dt*' may be given as;

$$dN = N \frac{[1-e^{(-\lambda t_1)}]}{e^{(\lambda t)}} dt \tag{4.5}$$

If the activity induced in the irradiated sample is recorded for time duration t_3, after a lapse time t_2, then the number of nuclei decayed in time interval between t_2 to (t_2+t_3) may be given as;

$$C = N\frac{[1-e^{(-\lambda t_1)}][1-e^{(-\lambda t_3)}]}{\lambda.e^{(\lambda t_2)}} \quad (4.6)$$

If the activity induced in the sample is recorded by a γ-ray spectrometer of efficiency G_ε, then absolute count rate 'C' and observed counting rate 'A' may be related as;

$$C = \frac{A}{\theta.K.G_\epsilon} \quad (4.7)$$

where, A is the total counts recorded during the accumulation time t_3 of the induced activity of decay constant λ, the term θ is the branching ratio of the characteristic γ-ray and $K=[\{1-exp(-\mu d)\}/\mu d]$ is the self-absorption correction factor for the material of the sample of thickness d (gm/cm^2) and of absorption coefficient μ (cm^2/gm) and G_ε the geometry dependent efficiency of the detector.

Thus, $\sigma_{X(a,b)}$ can be written as,

$$\sigma_{X(a,b)}(E) = \frac{A.\lambda\, e^{(\lambda t_2)}}{N_0.\Phi.\theta.K.G_\epsilon.[1-e^{(-\lambda t_1)}][1-e^{(-\lambda t_3)}]} \quad (4.8)$$

Also, the count-rate at the time of stop of irradiation $C_{t=0}$ can be given as,

$$C_{t=0} = \frac{A.\lambda\, e^{(\lambda t_2)}}{[1-e^{(-\lambda t_3)}]} \quad (4.9)$$

The reaction cross-section $\sigma_{X(a,b)}$ may be written with the help of above equations as,

$$\sigma_{X(a,b)}(E) = \frac{C_{t=0}}{N_0.\Phi.\theta.K.G_\epsilon.[1-e^{(-\lambda t_1)}]} \quad (4.10)$$

The cross-section for has been determined from the observed intensity of various γ-rays originating from the same residual nucleus and finally their weighted average has been taken. Reported cross-section values are the weighted average alongwith the

internal or external error whichever is larger. Following formulation has been used for determined the weighted average.

If $Y_1 \pm \Delta Y_1$, $Y_2 \pm \Delta Y_2$, $Y_3 \pm \Delta Y_3$, ……. are supposed to be the different measured values of the same quantity Y, then the weighted average is given as:

$$\bar{Y} = \frac{\sum W_i Y_i}{\sum W_i} \tag{4.11}$$

where, $$W_i = \frac{1}{(\Delta Y_i)^2} \tag{4.12}$$

$$\text{The internal error} = [\sum W_i]^{-1/2} \tag{4.13}$$

$$\text{The external error} = \left[\frac{\sum W_i(\bar{Y}-Y_i)^2}{n(n-1)\sum W_i}\right]^{-1/2} \tag{4.14}$$

Equation 4.13, depends entirely on the errors of individual observations, whereas equation 4.14, also depends upon the differences between observations from the mean value. External error is, therefore, a function of what might be called the external consistency of observation whereas; internal error depends upon the internal consistency.

A FORTRAN program EXP-SIGMA based on the equations 4.1 - 4.14, has been used for the determination of the neutron reaction cross-sections of the residues populated in $^{12}C+^{175}Lu$ at the respective irradiated energies. The errors quoted in the measured cross-section values are the internal or the external errors, whichever was greater. The experimentally measured cross-sections of identified in neutron reaction channels i.e. $^{184}Ir(3n)$, $^{183}Ir(4n)$ and $^{182}Ir(5n)$ is given in Table 4.2

Table 4.2: Experimentally measured production cross-sections for the neutron channels in $^{12}C+^{175}Lu$ system

Projectiles E_{lab} (MeV)	$^{184}Ir(3n)$	$^{183}Ir(4n)$	$^{182}Ir(5n)$
58.42±0.95	130±22.1	73.19±10.97	-
60.33±1.18	116.5±19.80	109±19.80	-
64.11±.80	110.6±18.80	345.75±51.86	-
66.23±.77	158.9±27.01	493.58±59.03	-
69.30±.70	78.8±13.39	557.78±53.66	30.14±4.52
71.17±1.31	40.4±6.86	497.00±59.55	119.33±17.90
73.49±1.02	46.4±7.9	510.99±76.64	334.23±50.13
76.40±0.9	18.92±3.14	379.34±56.90	478.11±71.71
78.36±1.08	21.2±3.60	289.47±43.42	528.87±79.33
80.70±1.3	10.27±1.74	196.86±29.52	667.59±100.13
83.20±0.8	6.28±1.06	159.85±23.972	731.50±109.7

4.3 Neutron reaction channels for $^{12}C+^{175}Lu$

The measurement and analysis of neutron reaction channels may be used to study the reaction mechanism involved in the production of reaction residues. In the present work, the three neutron channels viz $^{184}Ir(3n)$, $^{183}Ir(4n)$ and $^{182}Ir(5n)$ in the interaction of $^{12}C+^{175}Lu$ system at energies starting from the threshold to the ≈7Mev/A have been measured. The measured neutron channels have been analyzed within the framework of theoretical channels i.e. ALICE91 and PACE4 model.

In the first step the experimental cross section of the neutron reaction channels are compared with PACE4 predictions using the physically reasonable parameters and are shown in Fig 4.3-Fig 4.5. It has already been mentioned in the chapter 3 that in PACE4 calculations the level density parameter (a=A/K) is an important parameter

and by varying it one can reproduce the measured neutron residues. In the present work, the experimental data has been tested using three different values of free parameter viz k=8,9,10. For the sake of completeness the theoretical values calculated via PACE4 code at experimental analysis are tabulated in table 4.3 4.4 and 4.5

Table 4.3: PACE4 Calculations for ^{184}Ir cross section at three different level density parameter "K":

E_{lab} (MeV)	K=8	K=9	K=10
84	.114	.191	.153
82	.292	.401	.365
79.44	.546	.512	.888
77.3	.673	1.54	2.53
74.51	3.49	4.63	5.7
72.48	7.66	8.14	11.2
70	16.5	18.5	23.6
67	38.6	42.8	48.5
64.91	66.3	68.5	80.2
61.51	118	125	139
59.37	125	132	141
57.71	79.7	82.8	85.8

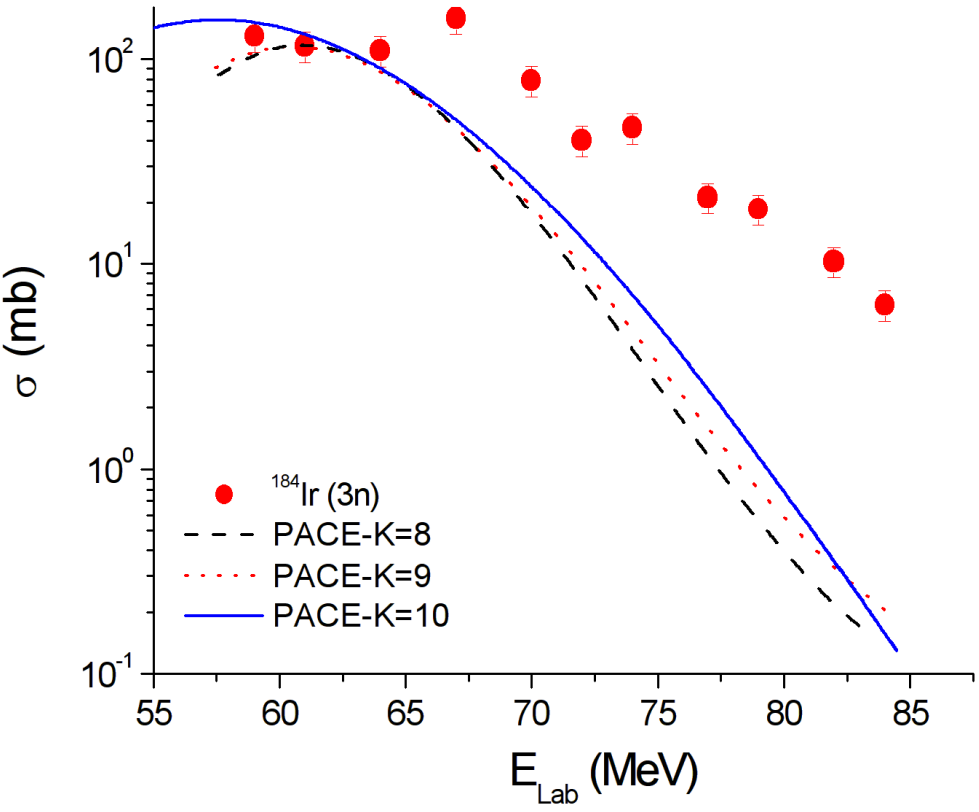

Figure 4.3: Experimental xn (x=3) channels populated in $^{12}C+^{175}Lu$ compared with PACE4 code at different k values

Table 4.4: PACE4 Calculations for ^{183}Ir cross section at three different level density parameter "K":

E_{lab} (MeV)	K=8	K=9	K=10
84	88.9	93.4	111
82	146	143	174
79.44	283	265	302
77.3	359	330	362
74.51	530	484	514
72.48	607	570	597
70	617	599	607
67	517	508	497
64.91	405	398	384
61.51	194	183	165
59.37	125	63	53.3
57.71	21.4	17.5	14.5

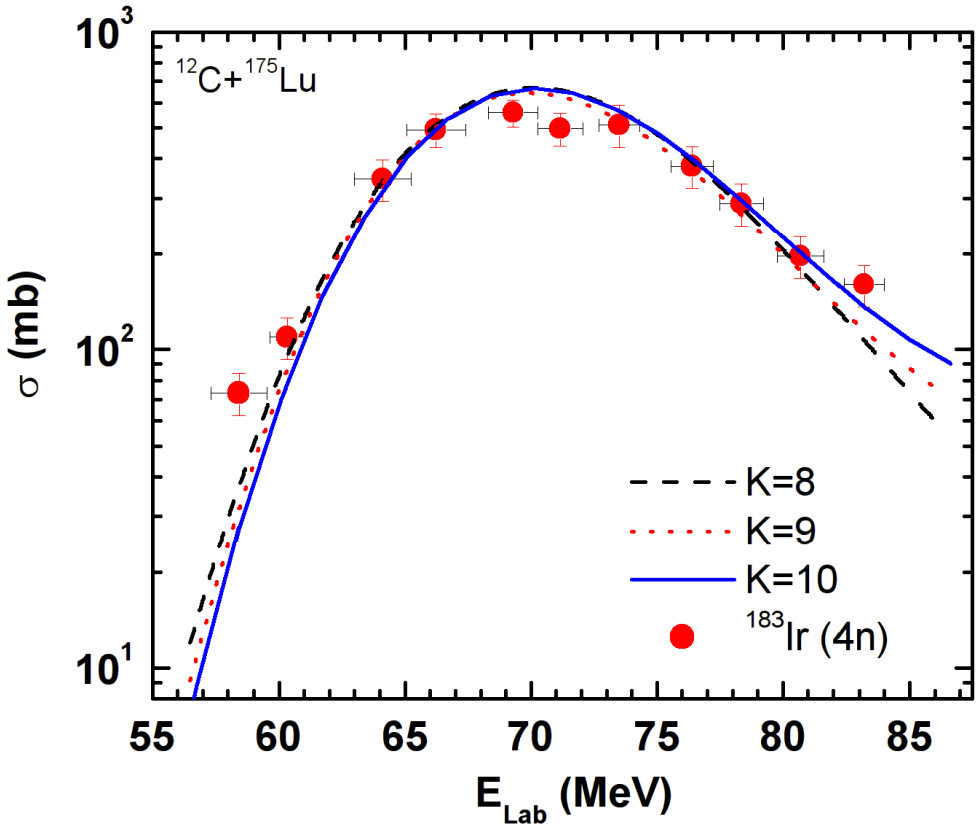

Figure 4.4: Experimental xn (x=4) channels populated in ^{12}C+^{175}Lu compared with PACE4 code at different k values

Table 4.5: PACE4 Calculations for ^{182}Ir cross section at three different level density parameter "K":

E_{lab} (MeV)	K=8	K=9	K=10
84	745	748	744
82	754	751	725
79.44	618	623	574
77.3	518	532	481
74.51	273	306	263
72.48	134	158	118
70	32.5	43.3	21.4
67	2.05	2.64	.783
64.91	.098	.23	.033
61.51	-	-	-
59.37	-	-	-
57.71	-	-	-

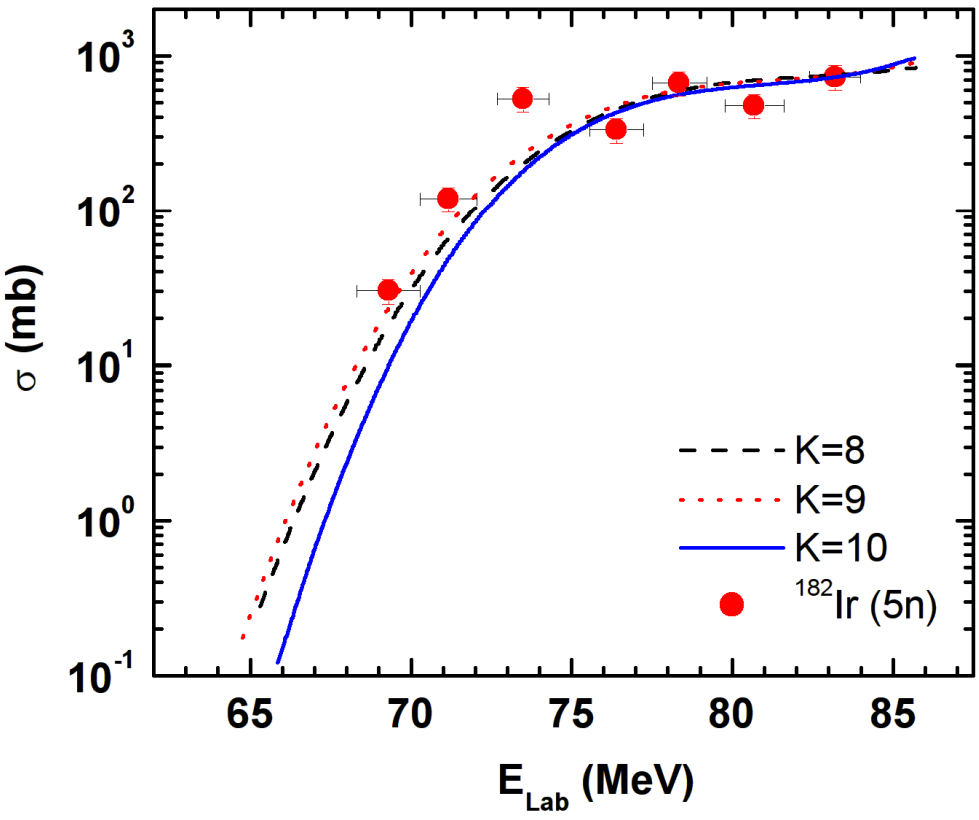

Figure 4.5: Experimental xn (x=5) channels populated in $^{12}C+^{175}Lu$ compared with PACE4 code at different k values

It may be pointed out that value of k>10, may give rise to the anomalous effects in particle multiplicity and compound nucleus temperature. As can be seen from the figure 4.4 and 4.5, theoretical calculations done by adopting the given set of parameters are found to agree reasonable well with the experimental results i.e. for 4n and 5n channels at K=10. However, for the experimental reaction channel ^{184}Ir(3n) (see fig 4.3) that the theoretical calculations agree well with the experimental data up to the peak position, but in the tail region at higher energies there is deviation of the experimental data. The higher values of experimental cross-sections in the tail region as compared to the PACE4 values may be attributed to the PE process, which is

dominant mode of reaction mechanism with reaction channels at relatively higher energies and is not considered in the PACE4 model.

It may be pointed out that the experimental data for other x channels, where x>3 occurring from ^{12}C with ^{175}Lu nuclei are satisfactorily reproduced (see fig 4.4 and 4.5) by PACE4 calculations using the same set of parameters indicating there is no contribution of PE emissions in higher nucleus evaporation channels. This is expected as PE emission is more likely in the first step of de-excitation and leaves the residual nucleus in an excited state from where emission of more neutrons is less likely. It may be pointed out that at relatively low energies there may not be enough energy available to have significant pre-equilibrium emission to end up with a total of 4 neutrons emitted, but if the energy is increased at some point the possibility of 4n channel exhibiting pre-equilibrium emission may also be observed. Since PE emission is not taken into account in the code PACE4, at relatively higher energies, which may be confirmed by comparing the measured neutron channels with the calculations done by the code ALICE-91.

In this code the compound nucleus calculations are done using the Weisskopf-Ewing model, while simulations for PE components are performed using geometry-dependent hybrid (GDH) model In the present calculations, the optical potentials of Becchetti and Greenlees have been used. The level densities of the residual nuclei may be calculated either from the Fermi gas model or from the constant temperature form. Although there are many parameters in this code, the level density parameter , the mean free path multiplier COST, and initial exciton number n_0 are some of the important parameters. The initial exciton number n_0 and mean free path multiplier COST govern mainly the pre-equilibrium components, while the level density parameter a affects mainly the equilibrium component. The level density parameter a is calculated from the expression a = A/K, where A is the mass number of the compound nucleus and K is an adjustable parameter. In the present calculations, the effect of variation of parameter K on measured EFs has also been studied. As a typical case, the experimentally measured and theoretically calculated $^{175}Lu(^{12}C,3n)^{184}Ir$ at two different values of K = 09 and 16 in ALICE-91

calculations are also shown in fig. 4.6. the theoretical cross-section at different COST and different K are tabulated in Table 4.6 which are calculated using ALICE91 for the $^{12}C+^{175}Lu$ system.

Table 4.6: Pre equilibrium cross-section calculated from the ALICE 91 code. "K" is the level density parameter. For cost see text.

E_{Lab} (KeV)	Compound Nucleus x-section	COST 1 K=9	COST 2 K=9	COST 3 K=9	COST 2 K=16
55	66.091	66.154	66.144	66.122	70.723
58	134.707	136.577	136.923	137.114	189.255
61	69.094	74.554	75.803	76.687	169.378
64	6.261	9.370	10.160	10.760	45.651
67	1.375	3.425	3.948	4.346	19.601
70	.531	2.367	2.830	3.179	12.196
73	.502	3.052	3.664	4.115	13.302
76	.100	1.586	1.938	2.194	6.014
79	.005	.396	.492	.562	1.353
82	.001	.234	.290	.330	.732
85	.000	.211	.260	.294	.600
88	.000	.194	.235	.262	.517

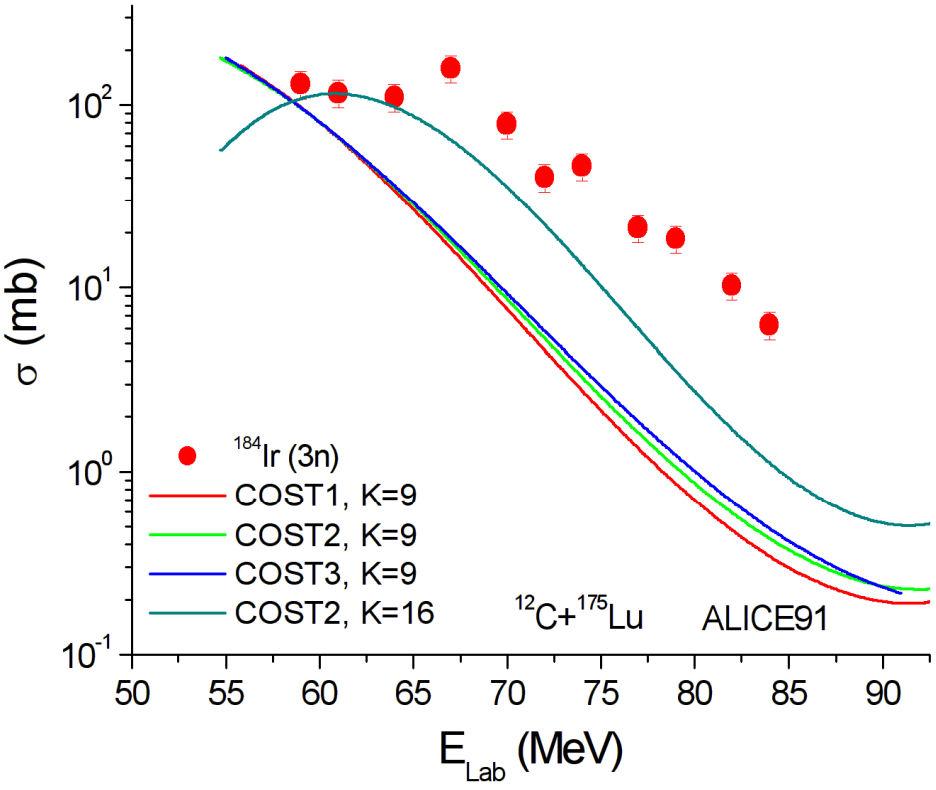

Figure 4.6: Experimental xn channel (i.e. 3n) populated in ^{12}C+^{175}Lu system compared with ALICE91 at different values of COST and K. The rotational energy is not included in the projectile energy.

When ALICE-91 calculations with the above mentioned values of parameters are compared with their experimental counterparts, it is observed that the maxima of the measured ^{184}Ir residue are at higher energies than those of the experimentally calculated. This is expected, since in ALICE-91 calculations the angular momentum effects have not been taken into account. In HI-induced reactions, the incident particle imparts relatively larger angular momentum to the composite system. If, in the last stages of nuclear de-excitation, higher angular momentum inhibits particle emission more than it does γ emission, then the peak of excitation function corresponding to the particle emission mode will be shifted to higher energies. The effect is more pronounced in HI reactions as compared to the light ion reactions, since the rotational

energy is much greater in the case of HI reactions. An estimate of the possible shift due to angular momentum effects may be made from the nuclear rotational energy. For a rigid body, the rotational energy is given by $E_{rot} \approx (m/M)E_{lab}$. Here, m/M is the ratio of the projectile and the target nucleus masses and E_{lab} is the incident energy. Since the angular momentum effects have not been considered in the Weisskopf-Ewing calculations of the present version of ALICE-91 code, it is desirable to shift the calculated excitation functions by the amount approximately equal to E_{rot} as calculated above. As such, in the present work, the calculated ^{184}Ir have been shifted by E_{rot} on the energy scale. The calculated ^{184}Ir residue with an energy shift equal to E_{rot} is shown in Fig. 4.7.

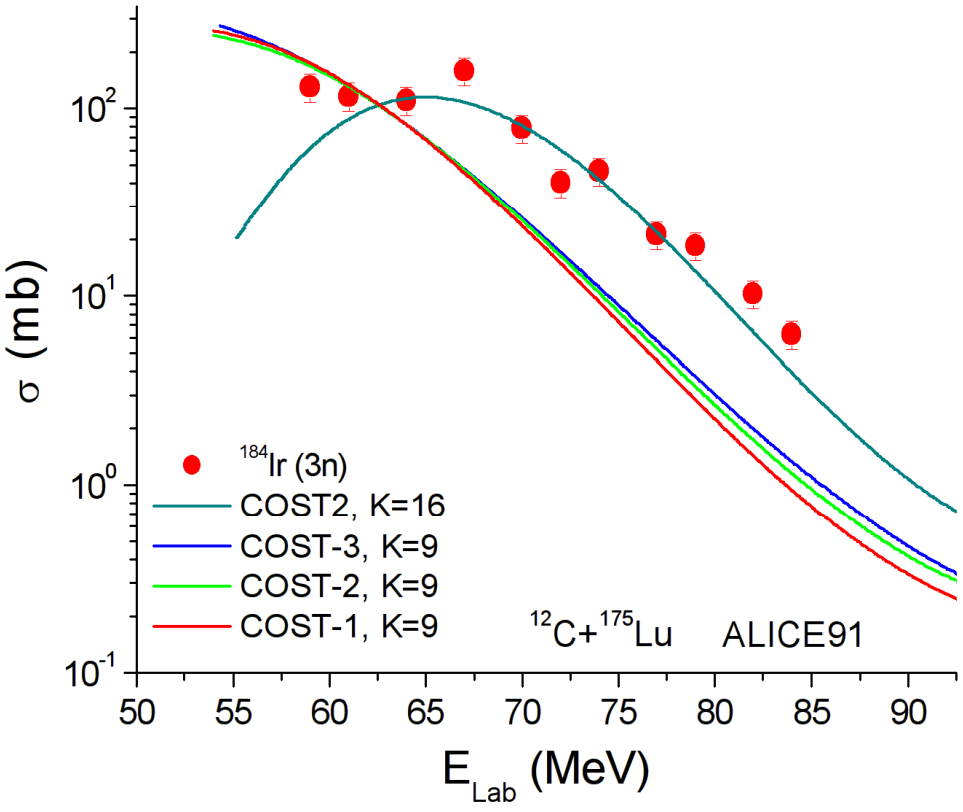

Figure 4.7: Experimental xn channel (i.e. 3n) populated in ^{12}C+^{175}Lu system compared with ALICE91 at different values of COST and K. The rotational energy is included in the projectile energy.

As observed from the figure, the theoretically calculated EF with K = 16 agrees satisfactorily well with the measured ones after incorporating rotational energy shifts for all cases, in general. Further, in code ALICE-91, the intermediate states of the system are characterized by the excitation energy E, number n_p of excited particles, and n_h of excited holes. Particles and holes are defined relative to the ground state of the nucleus and are called excitons. The initial configuration of the compound system defined by the exciton number $n_0 = (n_p + n_h)$ is an important parameter of PE formalism. In the present work, values of $n_0 = 12$ with configuration (6p + 6n) for 12C has been found to satisfactorily reproduce the experimental data, where p, and n represent the number of excited protons, and neutrons, respectively. The actual mean free path (MFP) inside the nucleus may be quite different from the one calculated using free nucleon-nucleon scattering data. In order to compensate for this difference, the parameter COST is provided in the code ALICE-91. A value of COST greater than zero means a smaller value of actual MFP for nucleon- nucleon scattering inside composite excited nucleus. As a representative case, the effect of variation of parameter COST on the calculated reaction residue ^{184}Ir (3n) is shown in figure.4.7. In the present work, a value of COST = 2 is found to reproduce the experimental data satisfactorily.

Chapter 5

CONCLUSIONS

Chapter 5

CONCLUSIONS

In the present work, the pre-equilibrium emission for the reaction $^{175}Lu(^{12}C,3n)^{184}I$ has been measured in the energy range starting from threshold to ≈7 MeV/A projectile energies. The analysis of the neutron channels indicates the presence of pre-equilibrium emission at such low energies. The theoretical calculations performed using the geometry-dependent hybrid (GDH) model of code ALICE-91 satisfactorily reproduce the measured excitation functions. It is observed that the high-energy tails of the measured ^{184}Ir or 3n-channel can't be explained by the pure compound nucleus mechanism and have significant contributions from PE emission. A precise measurement is required for better reproduction in terms of reaction processes viz. equilibrium and pre-equilibrium processes, of the experimentally measured channels in light-heavy ion induced reactions. As an extension of the work, in order to understand the dependence of pre-equlibrium processes on incident energy, mass asymmetry and target type, a large amount for neutron reaction channels for different projectile-target combinations are required.

References

1. N. Bohr, Nature, 137, 344 (1936).

2. S. N. Ghoshal, Phy. Rev. 80, 939 (1950).

3. Vijay R. Sharma, Abhishek yadav, Pushpendra P. Signh, Manoj K. Sharma, Devendra P. Singh, Unnati, Rakesh Kumar, K. S. Golda, B. P. Singh, A. K. Sinha and R. Prasad.

Phys. Rev. C. (2011), accepted for publication

4. Vijay R. Sharma, Abhishek yadav, Pushpendra P. Signh, Manoj K. Sharma, Devendra P. Singh, Unnati, Rakesh Kumar, K. S. Golda, B. P. Singh, A. K. Sinha and R. Prasad.

EPJ web of Conferences, published by EDP Sciences, 2011

5. G. K. Mehta and A. P. Patro; Nucl. Inst. and Meth. A268, 334 (1988).

6. B. P. Ajithkumar et. al.; Nucl. Inst. and Meth. A343, 327 (1994).

7. R. C. Kotch; Activation Analysis Handbook, Academic Press, New York and London, 1960.

8. James F. Ziegler, SRIM06; http://www.srim.org/

9. CANDLE: Data Acquisition and Analysis System designed to support the accelerator based experiments at the Inter University Accelerator Centre, New Delhi, India.

10. http://www.nndc.bnl.gov/ [For table of Isotopes]

11. E. Brown and R. B. Firestone, Table of Isotopes, Wiley, New York, 1986.

12. J. K. Tuli, Nuclear Wallet Card, National Nuclear Data Center, Brookhaven National Laboratory, Upton, New York, USA (2000).

13. Akira Iwamoto et al., journal of Nuclear Science and Technology 39 (4), 332-336 (2002).